Accepted Manuscript

Title: Treatment of olive oil mill wastewater by single electrocoagulation with different electrodes and sequential electrocoagulation/electrochemical Fenton-based processes

Authors: Nelly Flores, Enric Brillas, Francesc Centellas, Rosa María Rodríguez, Pere Lluís Cabot, José Antonio Garrido, Ignasi Sirés

PII: S0304-3894(17)30959-7
DOI: https://doi.org/10.1016/j.jhazmat.2017.12.059
Reference: HAZMAT 19091

To appear in: *Journal of Hazardous Materials*

Received date: 19-8-2017
Revised date: 24-11-2017
Accepted date: 21-12-2017

Please cite this article as: Flores N, Brillas E, Centellas F, Rodríguez RM, Cabot PL, Garrido JA, Sirés I, Treatment of olive oil mill wastewater by single electrocoagulation with different electrodes and sequential electrocoagulation/electrochemical Fenton-based processes, *Journal of Hazardous Materials* (2010), https://doi.org/10.1016/j.jhazmat.2017.12.059

Treatment of olive oil mill wastewater by single electrocoagulation with different electrodes and sequential electrocoagulation/electrochemical Fenton-based processes

Nelly Flores, Enric Brillas*, Francesc Centellas, Rosa María Rodríguez, Pere Lluís Cabot, José Antonio Garrido, Ignasi Sirés*

Laboratori d'Electroquímica dels Materials i del Medi Ambient, Departament de Química Física, Facultat de Química, Universitat de Barcelona, Martí i Franquès 1-11, 08028 Barcelona, Spain

* Corresponding author: *E-mail address*: i.sires@ub.edu (I. Sirés)

E-mail address: brillas@ub.edu (E. Brillas)

RESEARCH HIGHLIGHTS

- Optimum combination for single electrocoagulation (EC) of OOMW: Fe anode / Fe cathode
- EC at 3 mA cm^{-2} for 20 min yielded about 40% TOC reduction
- Sequential EC/EF and EC/PEF: similar performance at natural pH, but PEF superior at pH 3.0
- EC/PEF (pH 3.0, 25 mA cm^{-2}, 0.5 mM Fe^{2+}) better than single EF and PEF: 97.1% TOC decay
- Up to 18 cyclic and 27 aliphatic components in OOMW: persistence of linear aliphatic acids

Abstract

The treatment of olive oil mill wastewater (OOMW) by novel sequential processes involving electrocoagulation (EC) followed by electro-Fenton (EF) or photoelectro-Fenton (PEF) under UVA irradiation has been studied using a boron-doped diamond anode and an air-diffusion cathode for H_2O_2 electrogeneration. Their performance was monitored from the removal of total organic carbon (TOC), chemical oxygen demand, turbidity, total solids and total nitrogen, as well as from the energy consumption. Preliminary EC assays were performed with one pair of electrodes made of Al, Fe, AISI 304 or AISI 316L. The Fe/Fe cell showed the best performance, yielding 40% TOC decay in 20 min. Subsequent EF or PEF at natural pH 7.2 performed similarly, whereas PEF became superior at pH 3.0 due to the action of UVA photons. Comparison between EC/PEF and single EF or PEF at pH 3.0 and 25 mA cm^{-2} with 0.50 mM Fe^{2+} revealed the positive outcome of the sequential process, attaining 97.1% TOC abatement after 600 min. GC-MS analysis of the raw wastewater allowed identifying 18 cyclic and 27 aliphatic compounds, most of which could not be removed by EC. The final solutions in EC/EF and EC/PEF contained a large plethora of persistent long-chain aliphatic acids and alkanes.

Keywords: Electrocoagulation; Electro-Fenton; Olive oil mill wastewater; Photoelectro-Fenton; Sequential process

1. Introduction

According to the International Olive Oil Council, up to 95% of the olive trees cultivated worldwide is located in the Mediterranean region and hence, most of global olive oil production comes from Southern Europe and North Africa. During the processing of olive oil in mills, large volumes of effluents are generated, being estimated as more than 30 million cubic meters [1,2]. Olive oil mill wastewater (OOMW) is usually dark and contains very large contents of toxic components such as tannins, phenols and acid compounds, accounting for up to 37% of its total mass [3,4]. OOMW is environmentally hazardous, since its high organic matter content and turbidity cause poor light penetration and under-oxygenation in the event of uncontrolled release into water bodies [1,2]. It has been documented that OOMW may contain up to 150 g L^{-1} of total solids (TS), 170 g L^{-1} of 5-day biochemical oxygen demand (BOD_5) and 110 g L^{-1} of chemical oxygen demand (COD) [1-4]. Hence, these effluents must be decontaminated before discharge.

Biological treatments and membrane technologies have been widely used for OOMW treatment [5]. Larger decontamination has been found by coagulation-flocculation [6,7], ozonation [6,8,9] and advanced oxidation processes (AOPs) like catalytic wet oxidation [6,10], Fenton's reagent (H_2O_2/Fe^{2+} mixture) [6,7-9] and photocatalysis [6]. Electrochemical treatments have also shown good results regarding the removal of organic components. Among them, the most ubiquitous is electrocoagulation (EC), in which the colloidal and/or charged particles contained in the effluent are primordially removed by adsorption onto Fe(III) or Al(III) hydroxides generated upon anodic dissolution of Fe [11-13] or Al [11,13-15]. For a sample with COD = 48,500 mg L^{-1} and pH 6.2, Inan et al. [11] reported 42% and 52% of COD decrease after 30 min of EC at current density (j) = 20 mA cm^{-2} using sacrificial

Fe and Al anodes, respectively. Greater COD removal of ca. 75% was described by Abdhoum and Monser [14] for a similar sample with an Al anode at 75 mA cm^{-2} for 25 min.

EC mechanisms mainly allow phase separation, which causes the accumulation of organics in the sludge upon settling, thereby needing a post-treatment. Conversely, mineralization of OOMW components by hydroxyl radical (•OH) generated on site is feasible by electrochemical AOPs (EAOPs) like electrochemical oxidation (EO) [16-23] and electro-Fenton (EF) [24]. EO favors the degradation of organics mediated by the powerful •OH generated from water oxidation at the anode. This route competes with the degradation mediated by active chlorine (Cl_2/HClO/ClO^-), generated whenever the solution contains high Cl^- concentrations [25-27]. The actual performance of EO regarding COD removal depends on the initial organic load, the amount of present or added Cl^- and the anode nature. Thus, upon addition of Cl^-, 54%, 60%, 71% and 100% COD was removed at high current using Ti/RuO_2 [21], PbO_2 [22], Ti-Ta/Pt-Ir [20] and Ti/Pt [18] anodes, respectively. The use of a more powerful anode like boron-doped diamond (BDD) did not improve the performance, as shown for the treatment of an effluent with COD = 40,000 mg L^{-1} at 20 A for 15 h, which only yielded 19% COD decay with specific energy consumption of 96 kWh $(kg\ COD)^{-1}$ [23]. On the other hand, Bellakhal et al. [24] described the total mineralization of an OOMW sample by EF using a Pt/carbon-felt cell, where H_2O_2 was generated on site and a catalytic quantity of Fe^{2+} was added to produce •OH in the bulk from Fenton's reaction.

Few sequential processes that include electrochemical technology have been proposed to enhance OOMW degradation. Hanafi et al. [28] showed increasing biodegradability when treating a sample by EC with bipolar Al electrodes followed by biological process. Esfandyari et al. [29] used EC with Al anodes, with addition of NaCl and H_2O_2, followed by EO with a Ti/RuO_2 anode to finally obtain reductions of 96% COD, 94% BOD_5 and 89% turbidity. In a study by Cañizares et al. [30], COD content decreased to 700 mg L^{-1} using Fenton's reagent,

whereas the resulting recalcitrant wastewater was totally mineralized by EO with a BDD/stainless steel cell at high *j*. A sequential treatment including consecutive EF, anaerobic digestion and ultrafiltration has been developed by Khoufi et al. [31-33], reaching pilot plant scale. The overall process led to complete detoxification with an energy consumption of 73.5 kWh m^{-3}. Pretreatment of produced water by EC prior to reverse osmosis has also been reported [34].

Based on the positive results obtained in sequential treatment of OOMW, more research efforts are needed for further enhancement and scale-up. EC seems appropriate for a fast decay of the organic matter content in relatively short time, whereas subsequent treatment by electrochemical Fenton-based processes like EF and photoelectro-Fenton (PEF, under UVA irradiation) has not been tested yet. These latter powerful technologies could offer excellent perspectives for rapid and cost-effective decontamination.

This paper aims to assess the performance of novel sequential EC/EF and EC/PEF processes for OOMW treatment. Single EC was exhaustively investigated with Fe, Al and stainless steel (AISI 304 and 316L) electrodes at different *j* to optimize the pretreatment. Sequential treatments were made using optimum EC and subsequent EF or PEF of the supernatant liquid. The effect of pH and *j* was investigated to assess their oxidation power. Comparative single EF or PEF treatment of the conditioned OMWW at pH 3.0 was also made to demonstrate the benefits of technology coupling. The OOMW degradation in each assay was monitored from the change of parameters such as total organic carbon (TOC), COD, turbidity and specific energy consumption with electrolysis time.

2. Experimental

2.1. Chemicals

Sodium sulfate, heptahydrated ferrous sulfate and sulfuric acid (used to adjust the solution pH to 3.0) were of analytical grade provided by Fluka. and Acros Organics. All the analytic solutions were prepared with Millipore Milli-Q water of resistivity > 18 MΩ cm. Chemicals used for analysis were of HPLC or analytical grade provided by Merck and Panreac.

2.2. OOMW sample

The raw OOMW was withdrawn from a decanter that acted as a collector to receive wastewater from the cleaning tasks at a premium extra virgin olive oil production mill in northeastern Spain in October of 2016. It was kept at 4 ºC in a refrigerator and, before assays, the volume of required OOMW was conditioned by microfiltration with 45 μm cloth to remove the larger insoluble particles and to obtain stable physicochemical properties.

2.3. Electrolytic systems

All the electrolytic experiments were performed in an open, undivided, cylindrical glass cell of 200 mL capacity. The wastewater was vigorously stirred with a magnetic bar at 700 rpm and its temperature was kept to 25 ºC using thermostated water. The EC assays were performed with 150 mL of the OOMW sample at natural pH using one pair of electrode, chosen among Fe, Al, and stainless steel (AISI 304 and AISI 316L) plates. The geometric area of each electrode was 10 cm^2 and the interlectrode gap was 1 cm. The EF and PEF processes were made with 100 mL of wastewater, either conditioned or previously pretreated by EC. For sequential treatments, samples treated by EC were centrifuged with a NÜVE NF 120 centrifuge at 4100 rpm for 10 min, and the supernatant liquid was further treated by EF or PEF. The anode was a 3 cm^2 BDD thin-film on Si provided by NeoCoat and the cathode was a 3 cm^2 carbon-PTFE air-diffusion electrode provided by Sainergy Fuel Cell, with an interelectrode gap of about 1 cm. The cathode was mounted as described elsewhere [35] and was fed with air pumped at 1 L min^{-1} for continuous H_2O_2 generation. In some assays, a 3 cm^2

Pt foil (99.99% purity, SEMPSA) was used. The PEF process was ran under the same conditions as EF, but with irradiation using a Philips 6 W UVA lamp (λ_{max} = 360nm) of 5 W m^{-2} power density, as determined by a Kipp&Zonen CUV 5 UV radiometer. A constant *j* was provided by an EG&G Princeton Applied Research 273A potentiostat-galvanostat, whereas the cell voltage (E_{cell}) was monitored with a Demestres 601BR digital multimeter.

The metallic electrodes for EC were mechanically abraded with SiC paper, chemically cleaned with 0.1 M NaOH or H_2SO_4 solution and ultrasonically cleaned in Milli-Q water. The latter operation was repeated before each new trial. The surface of the BDD anode was initially cleaned via polarization in 100 mL of 0.050 M Na_2SO_4 at 100 mA cm^{-2} for 180 min.

2.4. Analytical methods

The main physicochemical characteristics of the OOMW sample were measured with: (i) a Crison GLP 22 pH-meter for pH; (ii) a Metrohm 644 conductometer for specific conductivity; (iii) a WTW TURB 55 IR turbidimeter for turbidity; (iv) TOC was obtained by filtering the sample with Whatman 0.45 μm PTFE filters followed by direct injection into a Shimadzu VCSN TOC analyzer; (v) total nitrogen (TN) was obtained through a TNM-1 module coupled to the TOC analyzer; (vi) cations concentration was determined by inductively coupled plasma with an Optima 3200RL spectrometer, and (vii) anions concentration was found by ion chromatography with a Kontron 465 LC fitted with a Waters IC-PAK (150 mm × 4.6 mm) anion-exchange column at 35 ºC and coupled to a Waters 432 conductivity detector. The mobile phase was an organic mixture at 2.0 mL min^{-1}. Other parameters were obtained following the Standard Methods [36]: (viii) COD with Hach Lange LCK014, LCK514 and LCK614 COD cuvette tests using a Hach DR 3900 UV–vis spectrophotometer (method 5220 D); (ix) BOD_5 with a WTW Oxitop 12 respirometric system using seed from a municipal wastewater treatment plant (method 5210 D); (x) TS upon evaporation and drying to constant weight at 103 ºC (method 2540 B); (xi) total dissolved

solids (TDS) after evaporation at 180 ºC, then reaching constant weight (method 2540 C); and (xii) volatile solids (VS) after treatment at 550 ºC to reach constant weight (method 2540 G).

Average data of duplicated trials are always reported. Good reproducible values were found with very small errors (< 2%) within 95% confidence interval and, for this reason, the corresponding error bars are not shown. The specific energy consumption per unit TOC mass (EC_{TOC}) for each experiment was calculated from [37]:

$$EC_{TOC}\ (\text{kWh (kg TOC)}^{-1}) = \frac{1000\, E_{cell}\, I\, t}{V\, \Delta(TOC)_{exp}} \quad (1)$$

where E_{cell} is in V, I is the applied current (in A), t is the electrolysis time (in h), V is the wastewater volume (in L) and $\Delta(TOC)_{exp}$ is the TOC removal (in mg L^{-1}). For PEF trials, Eq. (1) was utilized as well, without considering the electrical energy needed to power the UVA lamp, because it could be potentially replaced by free sunlight as previously shown [38,39].

Organic components of the conditioned OOMW and those in samples resulting from the treatments were identified by gas chromatography-mass spectrometry (GC-MS), being their mass spectra interpreted with a NIST05-MS library. Such components of about 100-130 mL samples were extracted out with 3 × 25 mL of dichloromethane (DCM) or ethyl acetate (EA). The resulting organic solution was dried over anhydrous Na_2SO_4, filtered and its volume reduced to 1 mL to be analyzed by GC-MS on an Agilent system with a 6890N GC and a 5975C MS (EI mode at 70 eV). The GC was fitted with either a polar HP INNOWax or non-polar Teknokroma Sapiens-X5ms column (0.25 μm, 30 m × 0.25 mm). The temperature ramp was 36 ºC (1 min) to 250 ºC or 325 ºC, respectively, at 5 ºC min^{-1}, with a hold time 10 min. The inlet, source and transfer line were 250, 230 and 250 ºC for the polar column, and 250, 230 and 300 ºC for the non-polar one.

3. Results and discussion

3.1. Characterization of the OOMW sample

The physicochemical characteristics of the raw OOMW after conditioning with 0.45 μm filters are summarized in Table 1. The sample presented: neutral pH; low conductivity; high TOC, COD, turbidity, TS, TDS and VS values; small BOD_5/COD ratio near 0.4 (low biodegradability); low TN content; prevalence of Na^+ over cations like K^+, Ca^{2+} and Mg^{2+}, being insignificant the iron concentration; and large predominance of SO_4^{2-} over smaller quantities of Cl^- and NO_3^- anions. Note that COD and TOC measurements include the oil content.

Table 2 summarizes the large variety of organic compounds identified for the conditioned OOMW by GC-MS, using DCM or EA as solvents for extraction and polar or non-polar columns for GC separation. Up to 18 cyclic and 27 aliphatic components were identified. The pre-eminent cyclic compounds were benzene derivatives with alkyl, alkoxy, hydroxyl, nitroso, aldehyde, amine and/or amide groups. The aliphatic products were: short-chain alcohols, diols and thiols; long-chain acids like oleic and octadecanoic along with short-chain ones like malic and acetic; and long-chain alkanes such as nonadecane, decane and eicosane. All these components confer a large complexity to the sample, being difficult its degradation.

3.2. EC treatment of the OOMW sample

A first series of comparative EC assays was performed with 150 mL of the conditioned sample using an Al, Fe, AISI 304 or AISI 316L anode of 10 cm^2 area. The cells contained the same cathode material and the experiments were prolonged for 45 min at 3, 10, 20 and 30 mA cm^{-2}, without pH regulation. Fig. 1a-d shows the normalized TOC-time plots and Fig. 2a-d depicts the corresponding EC_{TOC} vs. percentage of TOC removal. This representation is convenient when treating real wastewater since it informs about the energy consumption needed to reach a certain removal of organic carbon, thus limiting the waste of energy. Table

3 collects the final values of pH, conductivity, percentage of TOC, COD and turbidity removals, and EC_{TOC}.

Fig. 1a highlights that, at 3 mA cm^{-2}, TOC was gradually reduced in the Al/Al cell and slightly more rapidly in the Fe/Fe one, attaining 35.1% and 40.4% decontamination, respectively (see Table 3). Conversely, cells with AISI 304 or AISI 316L yielded similar but much slower TOC decay of 21.9% reduction (see Table 3). When *j* was increased to 30 mA cm^{-2}, TOC drop was faster in all cells, with removal ability rising in the sequence AISI 316L < AISI 304 << Al/Al ≤ Fe/Fe.

It is well-known that Al^{3+} and Fe^{2+} are released to the bulk from the sacrificial Al and Fe anodes through reactions (2) and (3) [40-42]. At the cathode, H_2 gas and OH^- are produced from reaction (4), which favors the formation of insoluble metallic hydroxides from reactions (5) and (6) [41,42].

$$Al_{(s)} \rightarrow Al^{3+}_{(aq)} + 3e^- \quad (2)$$

$$Fe_{(s)} \rightarrow Fe^{2+}_{(aq)} + 2e^- \quad (3)$$

$$2H_2O + 2e^- \rightarrow H_{2(g)} + 2OH^- \quad (4)$$

$$Al^{3+}_{(aq)} + 3H_2O \rightarrow Al(OH)_{3(s)} + 3H^+ \quad (5)$$

$$4Fe^{2+}_{(aq)} + 10H_2O + O_{2(g)} \rightarrow 4Fe(OH)_{3(s)} + 8H^+_{(aq)} \quad (6)$$

Reaction (6) shows that the initially generated Fe^{2+} is transformed into $Fe(OH)_3$ in presence of O_2 gas. The insoluble $Al(OH)_3$ and $Fe(OH)_3$ flocs with large surface area coagulate and remove pollutants by surface complexation or electrostatic attraction [41]. Moreover, organics can be reduced by Fe^{2+} in a Fe/Fe cell [42] and/or oxidized by active chlorine (Cl_2/HClO/ClO^-) formed from Cl^- oxidation at the anode [42,43]. The resulting byproducts may coagulate with the insoluble flocs enhancing the removal of organics.

The occurrence of reaction (3) in the Fe/Fe cell was confirmed from the loss of anode mass with electrolysis time at 30 mA cm^{-2}. A linear trend with slope of 5.39 mg Fe min^{-1} (R^2 = 0.998) was obtained, corresponding to n = 1.93, close to the expected two-electron oxidation of Fe.

The low TOC decay obtained in the two cells with stainless steels can be related to their smaller ability to produce insoluble $Fe(OH)_3$, since both alloys contain other metals (Cr, Ni, Mn and Mo). The oxidation of these anodes yields other soluble metallic ions apart from Fe^{2+} and their resistance to corrosion causes the consumption of part of the current in the oxidation of water to O_2. The larger extent of O_2 evolution at AISI 316L, with larger anti-corrosion ability, could explain the superiority of AISI 304 to remove more TOC at $j \geq 10$ mA cm^{-2} (see Fig. 1a).

Table 3 highlights that the final pH after EC treatment increased at greater j. This trend can be explained by the progressive accumulation of OH^- via reaction (4) due to the production of a smaller proportion of insoluble hydroxides. In contrast, the conductivity of the sample did not undergo any significant modification, suggesting a partial coagulation of salts with the hydroxide precipitates. Table 3 shows a variable relationship between the percentage of COD and TOC removals. TOC and COD inform about different characteristics of the components of OOMW. TOC accounts for the carbon of all organic compounds, whereas COD depends on their stability to oxidation by dichromate, which is determined by the molecule structure. The percentages for TOC and COD removals shown in Table 3 are a function of the kind of compounds removed in each EC run. Note also the large effect of EC on turbidity in all trials, with more than 99% abatement at $j \geq 10$ mA cm^{-2}.

An important parameter to know the viability of EC is its specific energy consumption. The change of EC_{TOC} with the percentage of TOC removal is depicted in Fig. 2a-d and the final value is found in Table 3. For both stainless steel anodes and each j, EC_{TOC} showed a

rapid growth with raising TOC removal, more evident with AISI 316L due to the lower TOC decay and higher E_{cell}. In contrast, the powerful Al/Al and Fe/Fe cells yielded a much lower and increase of EC_{TOC}. Comparison of Fig. 2a-d and data of Table 3 allows inferring that EC_{TOC} always grew at higher j, as expected by the progressively larger E_{cell}. From these results, the Fe/Fe cell was the most appropriate setup, entailing the lowest EC_{TOC} = 1.2 kWh (kg TOC)$^{-1}$ after 45 min of EC at 3 mA cm^{-2}. Similar values were obtained with the Al/Al cell up to 20 mA cm^{-2} (see Table 3).

The EC study was further extended to other 12 arrangements involving all combinations, aiming to assess the influence of the cathode material. Table 4 summarizes the values of pH, conductivity, percentages of TOC, COD and turbidity, as well as EC_{TOC} after 45 min of all treatments at 30 mA cm^{-2}. Results of Tables 3 and 4 evidence a notable influence of the cathode over TOC and COD removals, being more remarkable for EC_{TOC}. In contrast, the final pH was pre-eminently a function of the anode, meaning that it was regulated by the soluble and insoluble metallic species generated. A small change in conductivity was determined in all cases, corroborating the low adsorption salts onto flocs, whereas the turbidity almost completely disappeared. Regarding the TOC and COD abatement, the cells with Fe anode were the most effective, varying from 58.0% to 69.0% and from 60.9% to 65.0%, respectively. The lowest EC_{TOC} of 45.1 kWh (kg TOC)$^{-1}$ was also found for that cell, close to 46.8 kWh (kg TOC)$^{-1}$ for the Fe/AISI 304 one. The Al anode yielded greater EC_{TOC} values between 61.2 and 83.1 kWh (kg TOC)$^{-1}$. EC with AISI 304 and AISI 316L anodes was less efficient and more expensive.

3.3. Sequential EC/EF and EC/PEF treatment of the OOMW sample

The above EC study with the conditioned OOMW reveals the good performance of Fe/Fe cell. Since high j values led to a high pH and EC_{TOC}, with little enhancement of TOC and COD removals, the lowest j = 3 mA cm^{-2} was selected for sequential processes. From Fig. 1a,

a time of 20 min was chosen for the EC pretreatment because most TOC abatement (about 40%) was already reached. Table 5 shows the main characteristics of the resulting wastewater upon such an EC treatment, with a pH near 7.2. It contained 2.6 mg L^{-1} of total iron, which was assumed as sufficient for the subsequent EF or PEF treatment.

Fig. 3a depicts the normalized TOC decay with electrolysis time for the EC/EF tests. The EF post-treatment was made with 100 mL of the supernatant liquid from EC using a BDD/air-diffusion cell for 360 min. In EF, organics were mineralized by the competitive action of hydroxyl radical (•OH) produced at the anode surface from reaction (7) and in the bulk from Fenton's reaction (8) between electrogenerated H_2O_2 and Fe^{2+} formed during EC [25,44]. The latter reaction is ensured thanks to Fe^{2+} regeneration from cathodic reduction of Fe^{3+}.

$$BDD + H_2O \rightarrow BDD(^{\bullet}OH) + H^+ + e^- \quad (7)$$

$$H_2O_2 + Fe^{2+} \rightarrow Fe^{3+} + {}^{\bullet}OH + OH^- \quad (8)$$

The EF trials were carried out at 10 and 25 mA cm^{-2} at both, natural pH 7.2 and pH 3.0 after adjustment, since this is the optimal value [25,37,45,46]. Fig. 3a highlights a progressive TOC decay with time, being slower at long time because of the formation of more hardly oxidizable organics. At natural pH, TOC was reduced by 70.1% and 79.9% at 10 and 25 mA cm^{-2}, respectively, whereas at pH 3.0 slightly greater TOC abatements of 77.6% and 81.5% were found. The enhancement of TOC removal at greater *j* is due to the acceleration of reaction (7) and the generation of higher H_2O_2 amount from O_2 reduction at the cathode [37,38], thereby producing greater amounts of BDD(•OH) and •OH with the consequent faster mineralization. The little effect of pH on EF performance suggests the generation of relatively small quantities of •OH from Fenton's reaction (8), because of the small Fe^{2+} content after EC, being BDD(•OH) the prevailing oxidant.

As shown in Fig. 3b, lower energy consumptions resulted at smaller *j* and pH values. EC_{TOC} was 25.8 kWh (kg TOC)$^{-1}$ at pH 3.0 and 10 mA cm^{-2}, raising up to 110.9 kWh (kg TOC)$^{-1}$ at pH 7.2 and 25 mA cm^{-2} with similar TOC reduction. These results demonstrate that low *j* values at pH 3.0 in EF lead to a more viable sequential treatment.

Table 5 summarizes other relevant physicochemical parameters of the resulting wastewater after sequential treatment with EF at pH 7.2 and 25 mA cm^{-2}. It is noticeable the low BOD_5/COD ratio of 0.143, indicating a poor biodegradability, and the smaller removal of COD compared to TOC, suggesting the presence of highly recalcitrant organics. The turbidity removal attained was near 99%, whereas TS and TN were poorly removed compared to EC treatment. The loss in TN suggests the release of volatile *N*-products during EF. The total iron content in the wastewater did not vary substantially during the post-treatment.

Analogous sequential treatments with PEF were further made. A larger mineralization was expected because the UVA photons can promote: (i) generation of Fe^{2+} and $^{\bullet}OH$ from photolysis of photoactive $Fe(OH)^{2+}$ via reaction (9) and (ii) photolysis of some organics and byproducts like Fe(III)-carboxylate complexes from reaction (10) [25,45,46].

$$Fe(OH)^{2+} + h\nu \rightarrow Fe^{2+} + {}^{\bullet}OH \quad (9)$$

$$Fe(OOCR)^{2+} + h\nu \rightarrow Fe^{2+} + CO_2 + R^{\bullet} \quad (10)$$

Fig. 4a shows a similar trend for the EC/PEF assays compared to homologous EC/EF, although with higher TOC decay, achieving 80.1% at pH 7.2 and 25 mA cm^{-2}, and 80.2% and 86.3% at pH 3.0 and 10 and 25 mA cm^{-2}, respectively. This behavior is also reflected in the corresponding EC_{TOC} plots depicted in Fig. 4b, with final values of 119.1, 22.3 and 74.7 kWh (kg TOC)$^{-1}$, respectively. Table 5 reveals that analogous values for BOD_5/COD, percentage of COD, turbidity, TS and TN removals, and total iron were found after both EC/EF and EC/PEF. One can then conclude that there is little enhancement upon UVA irradiation

compared to EC at natural pH. In contrast, better TOC decays with lower EC_{TOC} were found at pH 3.0, probably due to the higher rate of reactions (9) and (10) enhancing the oxidation power of PEF.

An additional sequential assay was carried out using a Pt/air-diffusion cell in PEF, at pH 3.0 and 25 mA cm^{-2}. Fig. 4a and b show the low performance of this process, yielding 70.9% TOC abatement with EC_{TOC} = 68.3 kWh (kg TOC)$^{-1}$. Note that TOC was not practically reduced after 60 min of PEF with Pt,. This agrees with the higher oxidation ability of reactive BDD(•OH) compared to Pt(•OH) [25-28].

Samples resulting from EC, EC/EF and EC/PEF treatments shown in Table 5 were analyzed by GC-MS. Most of initial cyclic components of Table 1 were detected after EC, along with other phenol and benzenamine derivatives arising from the cleavage of adsorbed molecules onto $Fe(OH)_3$. Further EF or PEF removed most of these organics, only remaining some hydroxylated derivatives like 3,5-dihydroxytoluene, 4-hydroxybenzeneacetic acid and 2-hydroxy-5-methylbenzaldehyde, formed upon attack of hydroxyl radicals. The fate of aliphatic compounds like oleic, hexadecanoic, decanoic and 4-hexenoic acids, dodecanamide and eicosane was very different because they persisted after EC and were still found after EF and PEF due to their slow destruction by hydroxyl radicals.

3.4. Comparison with single EF and PEF treatments

To check the viability of the sequential processes compared to the single ones, the conditioned OOMW was treated directly by EF and PEF. These trials were carried out at the optimum pH 3.0 with addition of 0.50 mM Fe^{2+} using the BDD/air-diffusion cell at 25 mA cm^{-2} for 600 min to attain a large mineralization. They were compared with an EC/PEF treatment, operating PEF at pH 3.0 and 25 mA cm^{-2} with 0.50 mM Fe^{2+}.

Fig. 5a depicts that single EF and PEF led to 74.2% and 87.1% mineralization, respectively. This demonstrates that generated BDD(•OH) and •OH radicals can oxidize many

organic pollutants in EF. The higher TOC decay in PEF indicates a positive action of UVA light to photolyze and mineralize photosensitive products. However, TOC was much more largely destroyed upon EC/PEF treatment, reaching 97.1% decontamination. This is a remarkable result, demonstrating that the almost total mineralization of the OOMW components that persist upon EC is feasible by a sequential treatment, which cannot be reached by single PEF. The addition of 0.50 mM Fe^{2+} at pH 3.0 accelerated Fenton's reaction (8). For example, after 360 min of PEF at pH 3.0 and 25 mA cm^{-2}, TOC was abated by 86.3% (see Fig. 4a) and 91.8% (see Fig. 5a) without and with Fe^{2+} addition, respectively. The EC_{TOC} profiles of Fig. 5b evidence maximum values of 196.1 and 126.2 kWh $(kg\ TOC)^{-1}$ after about 35%-45% TOC removal in EF and PEF. These values finally dropped to 155.1 and 108.3 kWh $(kg\ TOC)^{-1}$ as a result of the quicker TOC decay, probably due to the progressive formation of less refractory products to $^{\bullet}OH$ attack in the bulk. The EC_{TOC} of PEF was similar to 115.8 kWh $(kg\ TOC)^{-1}$ found in EC/PEF, but much greater TOC decay was attained in the sequential treatment. The long time required is due to the large recalcitrance of oil and other organic pollutants of the OOMW sample, but the low energy consumption per unit TOC mass makes the sequential treatment quite interesting for OOMW treatment.

4. Conclusions

The Fe/Fe cell performed better than the others for the EC treatment of OOMW. A j = 3 mA cm^{-2} for 20 min during EC pretreatment yielded about 40% TOC reduction without significant pH change and accumulating 2.61 mg L^{-1} of total iron. TOC decays and EC_{TOC} were quite similar after EF or PEF post-treatments at natural pH with a BDD/air-diffusion cell at 10 or 25 mA cm^{-2}, whereas PEF outperformed EF at pH 3.0 due to the potent photolytic action of UVA light. The sequential EC/PEF with addition of 0.50 mM Fe^{2+} at pH 3.0 and 25 mA cm^{-2} led to 97.1% TOC drop, much higher than in single EF or PEF, thus being more

efficient and viable for OOMW treatment. Long-chain linear aliphatic acids and alkanes were the most persistent organics in sequential treatments.

Acknowledgements

The authors thank financial support from project CTQ2016-8616-R (AEI/FEDER, EU) and the PhD fellowship awarded to N. Flores by SENESCYT (Ecuador).

References

[1] S. Magdich, C. Ben Ahmed, R. Jarboui, B. Ben Rouina, M. Boukhris, E. Ammar, Dose and frequency dependent effects of olive mill wastewater treatment on the chemical and microbial properties of soil, Chemosphere 93 (2013) 1896-1903.

[2] S. Dermeche, M. Nadour, C. Larroche, F. Moulti-Mati, P. Michaud, Olive mill wastes: Biochemical characterizations and valorization strategies, Process Biochem. 48 (2013) 1532-1552.

[3] M. DellaGreca, L. Previtera, F. Temussi, A. Zarrelli, Low-molecular-weight components of olive oil mill waste-waters, Phytochem. Anal. 15 (2004) 184-188.

[4] J.M. Ochando-Pulido, M.D. Victor-Ortega, G. Hodaifa, A. Martinez-Ferez, Physicochemical analysis and adequation of olive oil mill wastewater after advanced oxidation process for reclamation by pressure-driven membrane technology, Sci. Total Environ. 503-504 (2014) 113-121.

[5] N. Gholamzadeh, M. Peyravi, M. Jahanshahi, Study on olive oil wastewater treatment: Nanotechnology impact, J. Water Environ. Nanotechnol. 1 (2016) 145-161.

[6] J.M. Ochando-Pulido, S. Pimentel-Moral, V. Verardo, A. Martinez-Ferez, A focus on advanced physico-chemical processes for olive mill wastewater treatment, Sep. Purif. Technol. 179 (2017) 161-174.

[7] B.H. Gursoy-Haksevenler, I. Arslan-Alaton, Profiling olive oil mill wastewater by resin fractionation: Effect of acid cracking, coagulation, electrocoagulation, and Fenton's reagent, Clean: Soil, Air, Water 42 (2014) 1384-1392.

[8] P. Cañizares, J. Lobato, R. Paz, M.A. Rodrigo, C. Sáez, Advanced oxidation processes for the treatment of olive-oil mills wastewater, Chemosphere 67 (2007) 832-838.

[9] P. Cañizares, R. Paz, C. Sáez, M.A. Rodrigo, Costs of the electrochemical oxidation of wastewaters: A comparison with ozonation and Fenton oxidation processes, J. Environ. Manage. 90 (2008) 410-420.

[10] D. Pham Minh, P. Gallezot, S. Azabou, S. Sayadi, M. Besson, Catalytic wet air oxidation of olive oil mill effluents, Appl. Catal. B: Environ. 84 (2008) 749-757.

[11] H. Inan, A. Dimoglo, H. Simsek, M. Karpuzcu, Olive oil mill wastewater treatment by means of electro-coagulation, Sep. Purif. Technol. 36 (2004) 23-31.

[12] S. Khoufi, F. Feki, S. Sayadi, Detoxification of olive mill wastewater by electrocoagulation and sedimentation processes, J. Hazard. Mater. 142 (2007) 58-67.

[13] C. An, G. Huang, Y. Yao, S. Zhao, Emerging usage of electrocoagulation technology for oil removal from wastewater: A review, Sci. Total Environ. 579 (2016) 537-556.

[14] N. Adhoum, L. Monser, Decolourization and removal of phenolic compounds from olive mill wastewater by electrocoagulation, Chem. Eng. Process. 43 (2004) 1281-1287.

[15] F. Hanafi, O. Assobhei, M. Mountadar, Detoxification and discoloration of Moroccan olive mill wastewater by electrocoagulation, J. Hazard. Mater. 174 (2010) 807-812.

[16] C. Belaid, M. Kallel, M. Khadhraou, G. Lalleve, B. Elleuch, J.-F. Fauvarque, Electrochemical treatment of olive mill wastewaters: Removal of phenolic compounds and decolourization, J. Appl. Electrochem. 36 (2006) 1175-1182.

[17] E. Kotta, N. Kalogerakis, D. Mantzavinos, The effect of solids on the electrochemical treatment of olive mill effluents, J. Chem. Technol. Biotechnol. 82 (2007) 504-511.

[18] S. Kul, R. Boncukcuoglu, A.E. Yilmaz, B.A. Fil, Treatment of olive mill wastewater with electro-oxidation method, J. Electrochem. Soc. 162 (2015) G41-G47.

[19] M. Gotsi, N. Kalogerakis, E. Psillakis, P. Samaras, D. Mantzavinos, Electrochemical oxidation of olive oil mill wastewaters, Water Res. 39 (2005) 4177-4187.

[20] A. Giannis, M. Kalaitzakis, E. Diamadopoulos, Electrochemical treatment of olive mill wastewater, J. Chem. Technol. Biotechnol. 82 (2007) 663-671.

[21] N. Papastefanakis, D. Mantzavinos, A. Katsaounis, DSA electrochemical treatment of olive mill wastewater on Ti/RuO_2 anode, J. Appl. Electrochem. 40 (2010) 729-737.

[22] F. Ghanbari, M. Moradi, F. Mehdipour, F. Gohari, Simultaneous application of copper and PbO_2 anodes for electrochemical treatment of olive oil mill wastewater, Desalination Water Treat. 57 (2016) 5828-5836.

[23] E. Chatzisymeon, N.P. Xekoukoulotakis, E. Diamadopoulos, A. Katsaounis, D. Mantzavinos, Boron-doped diamond anodic treatment of olive mill wastewater: Statistical analysis, kinetic modeling and biodegradability, Water Res. 43 (2009) 3999-4009.

[24] N. Bellakhal, M.A. Oturan, N. Oturan, M. Dachraoui, Olive oil mill wastewater treatment by the electro-Fenton process, Environ. Chem. 3 (2006) 345-349.

[25] E. Brillas, I. Sirés, M.A. Oturan, Electro-Fenton process and related electrochemical technologies based on Fenton's reaction chemistry. Chem. Rev. 109 (2009) 6570-6631.

[26] I. Sirés, E. Brillas, M.A. Oturan, M.A. Rodrigo, M. Panizza, Electrochemical advanced oxidation processes: today and tomorrow, Environ. Sci. Pollut. Res. 21 (2014) 8336-8367.

[27] F.C. Moreira, R.A.R. Boaventura, E. Brillas, V.J.P. Vilar, Electrochemical advanced oxidation processes: A review on their application to synthetic and real wastewaters, Appl. Catal. B: Environ. 202 (2017) 217-261.

[28] F. Hanafi, A. Belaoufi, M. Mountadar, O. Assobhei, Augmentation of biodegradability of olive mill wastewater by electrochemical pre-treatment: Effect on phytotoxicity and operating cost, J. Hazard. Mater. 190 (2011) 94-99.

[29] Y. Esfandyari, Y. Mahdavi, M. Seyedsalehi, M. Hoseini, G.H. Safari, M.G. Ghozikali, H. Kamani, J. Jaafari, Degradation and biodegradability improvement of the olive mill wastewater by peroxi-electrocoagulation/electrooxidation-electroflotation process with bipolar aluminum electrodes, Environ. Sci. Pollut. Res. 22 (2015) 6288-6297.

[30] P. Cañizares, L. Martínez, R. Paz, C. Sáez, J. Lobato, M.A. Rodrigo, Treatment of Fenton-refractory olive oil mill wastes by electrochemical oxidation with boron-doped diamond anodes, J. Chem. Technol. Biotechnol. 81 (2006) 1331-1337.

[31] S. Khoufi, F. Aloui, S. Sayadi, Treatment of olive oil mill wastewaters by combined process electro-Fenton reaction and anaerobic digestion, Water Res. 40 (2006) 2007-2016.

[32] S. Khoufi, F. Feki, F. Aloui, S. Sayadi, Pilot-plant results of the electro-Fenton treatment of olive mill wastewater followed by anaerobic digestion, Water Sci. Technol. 55 (2007) 259-265.

[33] S. Khoufi, F. Aloui, S. Sayadi, Pilot scale hybrid process for olive mill wastewater treatment and reuse, Chem. Eng. Process. 48 (2009) 643-650.

[34] S. Zhao, G. Huang, G. Cheng, Y. Wang, H. Fu, Hardness, COD and turbidity removals from produced water by electrocoagulation pretreatment prior to reverse osmosis membranes, Desalination 344 (2014) 454-462.

[35] J.R. Steter, E. Brillas, I. Sirés, I., On the selection of the anode material for the electrochemical removal of methylparaben from different aqueous media. Electrochim. Acta 222 (2016) 1464-1474.

[36] A.D. Eaton, L.S. Clesceri, E.W. Rice, A.E. Greenberg (Eds.), Standard Methods for the Examination of Water and Wastewater, 21 st ed., American Public Health Association (APHA), American Water Works Association (AWWA), Water Environment Federation (WEF), Washington D.C., USA, 2005.

[37] E.J. Ruiz, A. Hernández-Ramírez, J.M. Peralta-Hernández, C. Arias, E. Brillas, Application of solar photoelectro-Fenton technology to azo dyes mineralization: Effect of current density, Fe^{2+} and dye concentration, Chem. Eng. J. 171 (2011) 385-392.

[38] C. Flox, J.A. Garrido, R.M. Rodríguez, P.L. Cabot, F. Centellas, C. Arias, E. Brillas, Mineralization of herbicide mecoprop by photoelectro-Fenton with UVA and solar light, Catal. Today 129 (2007) 29-36.

[39] A. Thiam, I. Sirés, E. Brillas, Treatment of a mixture of food color additives (E122, E124 and E129) in different water matrices by UVA and solar photoelectro-Fenton, Water Res. 81 (2015) 178-187.

[40] V. Khandegar, A.K. Saroha, Electrocoagulation for the treatment of textile industry effluent--a review, J. Environ. Manage. 128 (2013) 949-963.

[41] A. Thiam, M. Zhou, E. Brillas, I. Sirés, Two-step mineralization of Tartrazine solutions: Study of parameters and by-products during the coupling of electrocoagulation with electrochemical advanced oxidation processes, Appl. Catal. B: Environ. 150-151 (2014) 116-125.

[42] E. Brillas, C.A. Martínez-Huitle, Decontamination of wastewaters containing synthetic organic dyes by electrochemical methods. An updated review, Appl. Catal. B: Environ. 166-167 (2015) 603-643.

[43] E. Bocos, E. Brillas, M.A. Sanromán, I. Sirés, Electrocoagulation: Simply a phase separation technology? The case of bronopol compared to its treatment by EAOPs, Environ. Sci. Technol. 50 (2016) 7679-7686.

[44] A. Dirany, I. Sirés, N. Oturan, A. Özcan, M.A. Oturan, Electrochemical treatment of the antibiotic sulfachloropyridazine: Kinetics, reaction pathways, and toxicity evolution. Environ. Sci. Technol. 46 (2012) 4074-4082.

[45] A. El-Ghenymy, N. Oturan, M.A. Oturan, J.A. Garrido, P.L. Cabot, F. Centellas, R.M. Rodríguez, E. Brillas, Comparative electro-Fenton and UVA photoelectro-Fenton degradation of the antibiotic sulfanilamide using a stirred BDD/air-diffusion tank reactor, Chem. Eng. J. 234 (2013) 115-123.

[46] H. Olvera-Vargas, N. Oturan, M.A. Oturan, E. Brillas, Electro-Fenton and solar photoelectro-Fenton treatments of the pharmaceutical ranitidine in pre-pilot flow plant scale, Sep. Purif. Technol. 146 (2015) 127-135.

Figure captions

Fig. 1. Normalized TOC decay with electrolysis time for the electrocoagulation (EC) treatment of 150 mL of conditioned OOMW at natural pH 6.9 and 25 ºC. Current density: (a) 3, (b) 10, (c) 20 and (d) 30 mA cm^{-2}. The cell contained two 10 cm^2 plates of the same material: (●) Al, (■) Fe, and stainless steel (▲) AISI 304 and (▼) AISI 316L.

Fig. 2. Specific energy consumption per unit TOC mass vs. percentage of TOC removal for the assays of Fig. 1.

Fig. 3. (a) Normalized TOC removal vs. electrolysis time and (b) specific energy consumption per unit TOC mass with percentage of TOC removal for sequential EC/electro-Fenton (EF) treatment of conditioned OOMW. (◆) Average profile for EC of 150 mL sample for 20 min with Fe/Fe cell at 3 mA cm^{-2} and 25 ºC. EF post-treatment with 100 mL of the supernatant solution after EC, using a BDD/air-diffusion cell of 3 cm^2 electrode area at 10 mA cm^{-2} and pH: (●) 7.2 and (■) 3.0, and 25 mA cm^{-2} at pH: (▲) 7.2 and (▼) 3.0. Temperature: 25 ºC.

Fig. 4. (a) Normalized TOC decay with electrolysis time and (b) specific energy consumption per unit TOC mass vs. percentage of TOC removal for sequential EC/photoelectro-Fenton (PEF) process of conditioned OOMW. (◆) Average profile for EC under the same conditions of Fig. 3. PEF post-treatment made like EF of Fig. 3, under irradiation with a 6 W UVA lamp, at 25 ºC using a: (▼) Pt/air-diffusion cell at pH 3.0 and 25 mA cm^{-2} or BDD/air-diffusion one at (▲) pH 3.0 and 10 mA cm^{-2}, (■) pH 7.2 and 25 mA cm^{-2}, and (●) pH 3.0 and 25 mA cm^{-2}.

Fig. 5. (a) Normalized TOC vs. electrolysis time and (b) specific energy consumption per unit TOC mass with percentage of TOC decay for the degradation of conditioned OOMW with a BDD/air-diffusion cell by (▲) EF and (●) PEF, both in 0.050 M Na_2SO_4 with 0.50 mM Fe^{2+}

at pH 3.0, 25 mA cm^{-2} and 25 ºC. (□) EC treatment as in Fig. 3, followed by (■) PEF of 100 mL of the supernatant solution with 0.50 mM Fe^{2+} at pH 3.0, 25 mA cm^{-2} and 25 ºC.

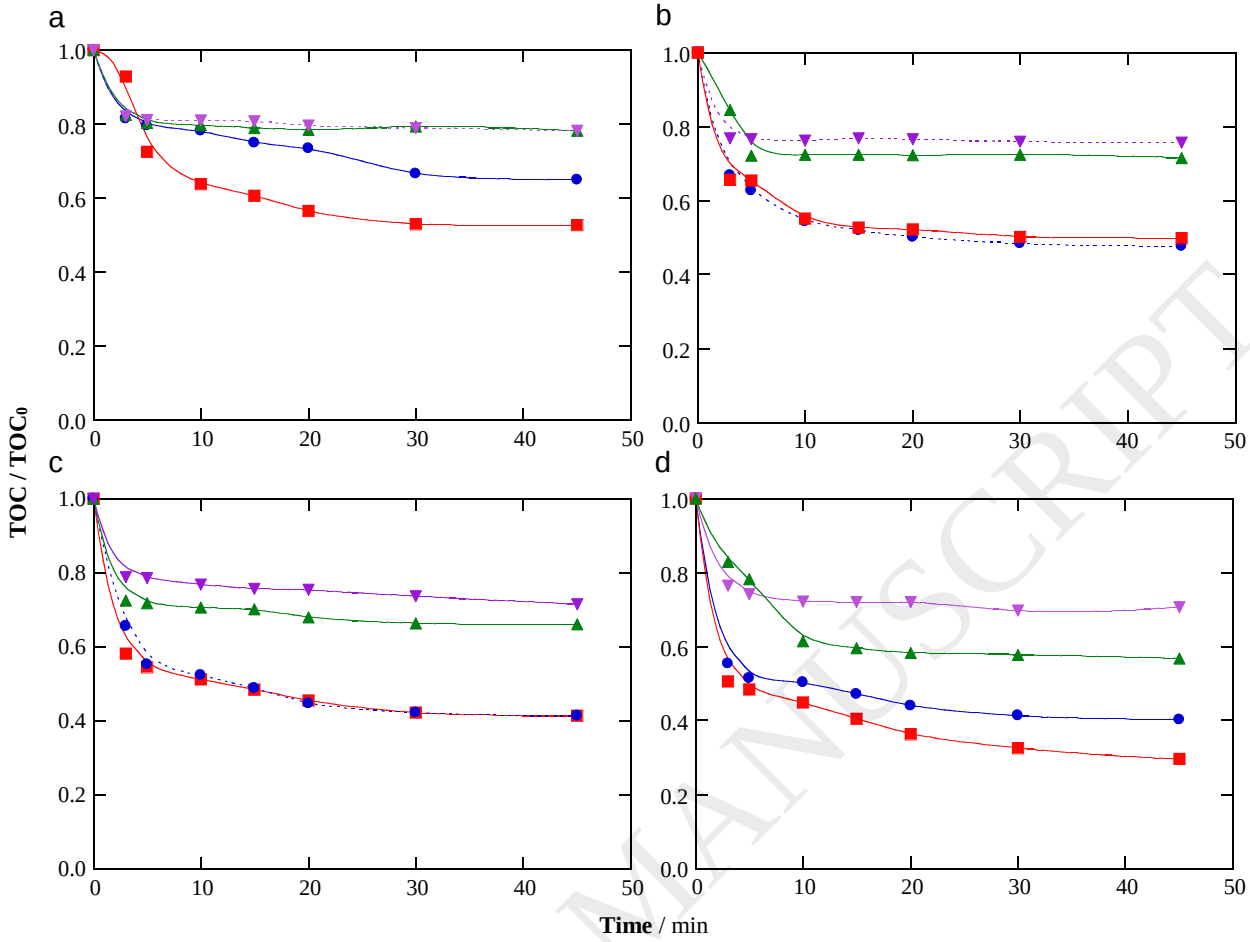

Fig. 1

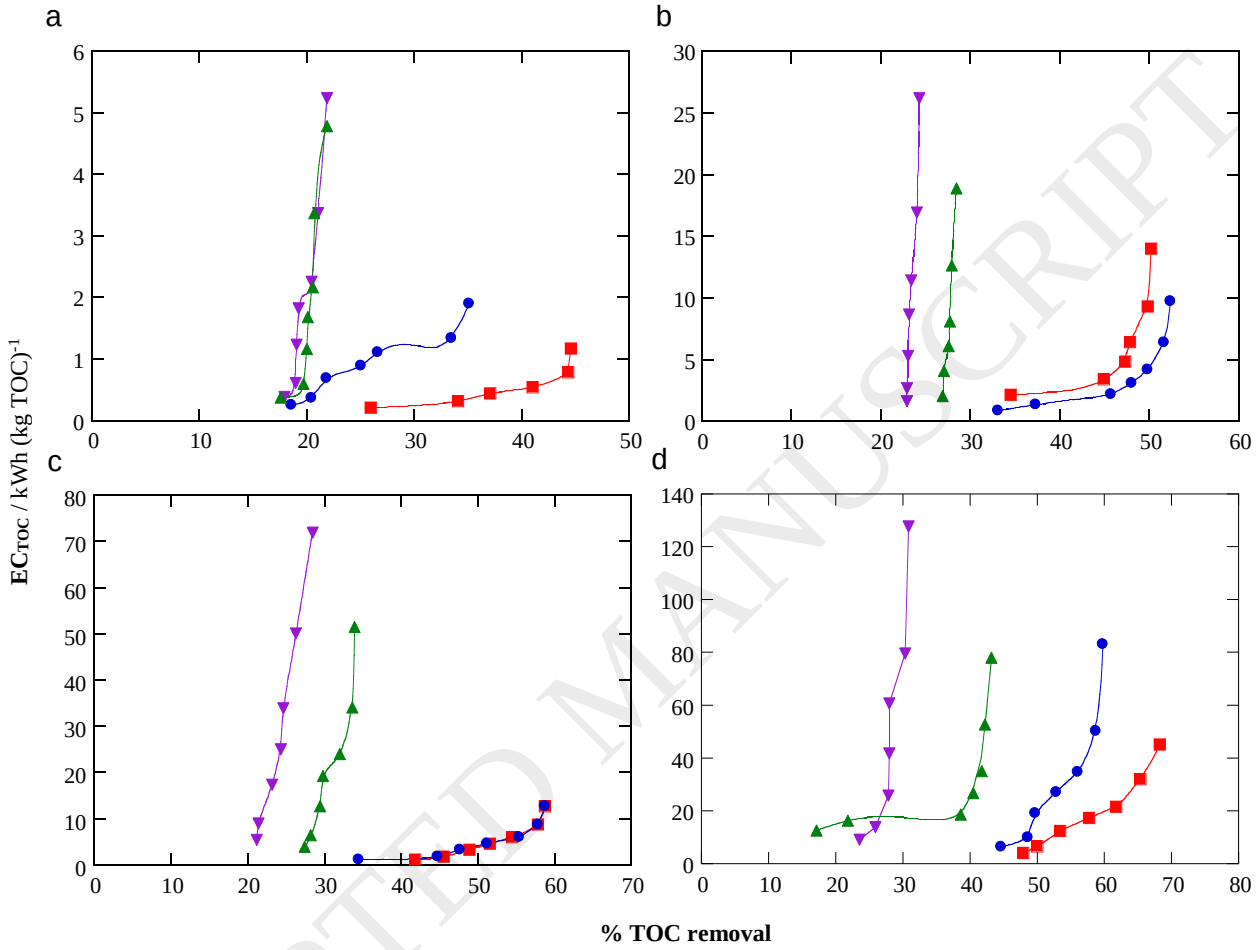

Fig. 2

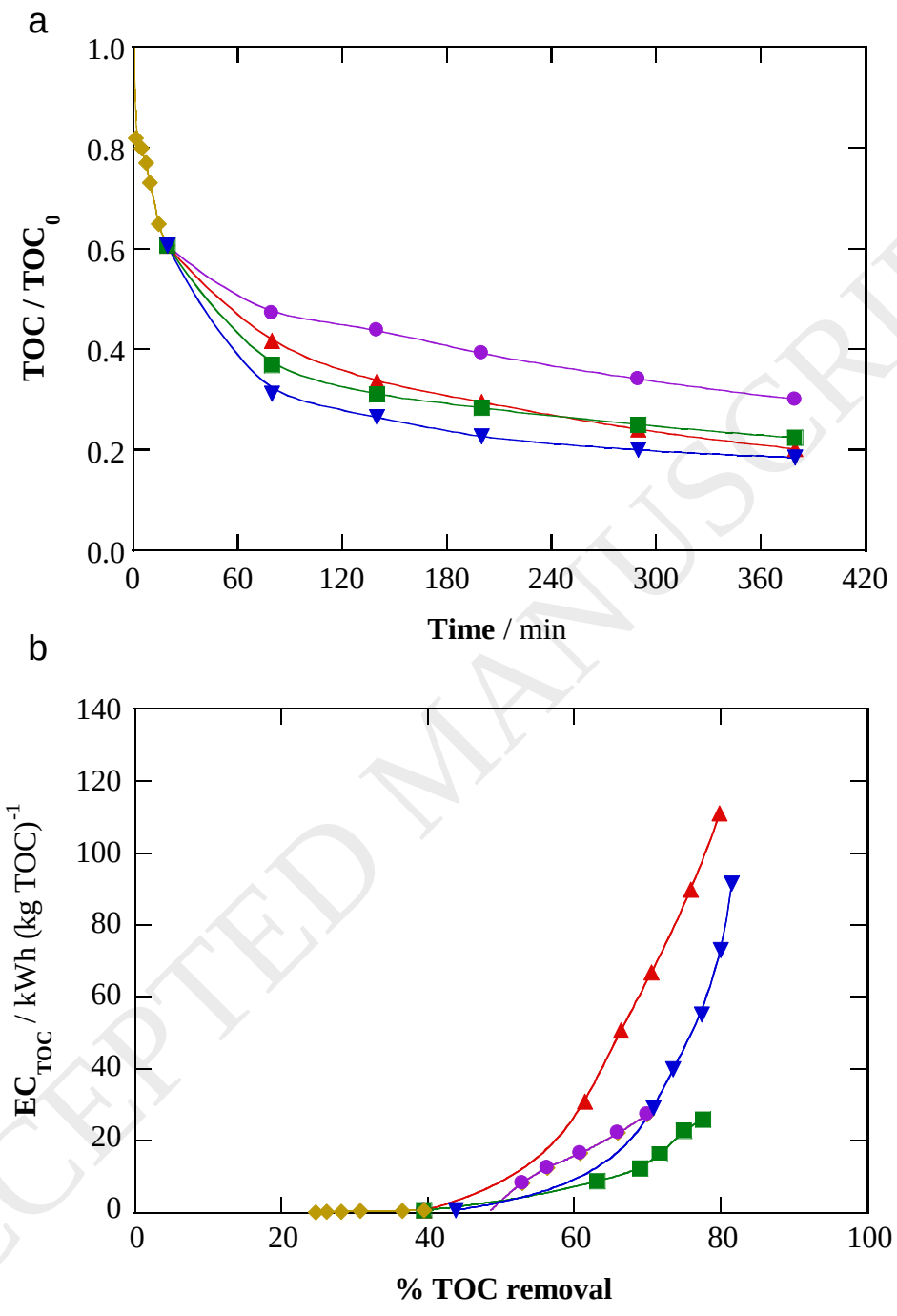

Fig. 3

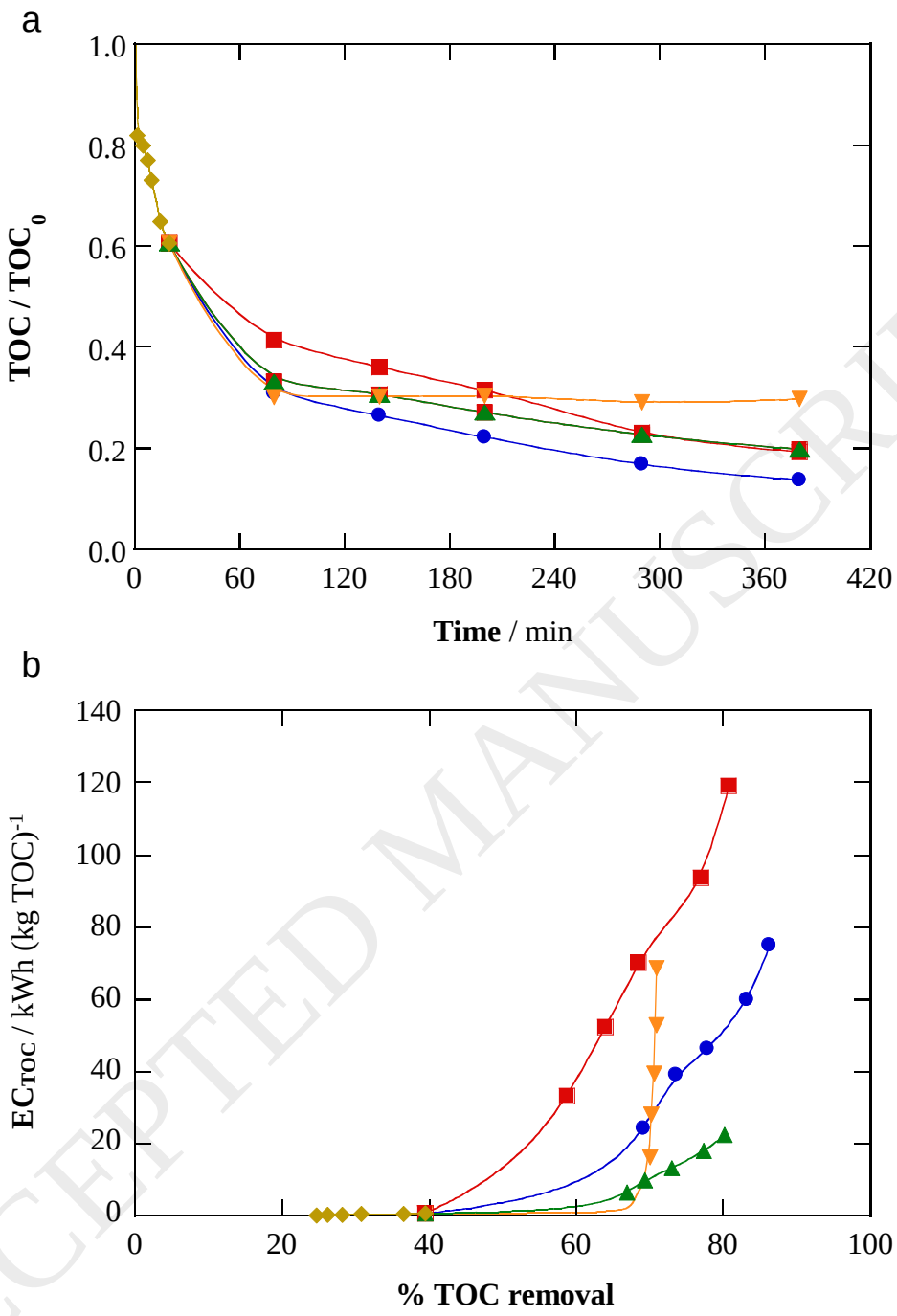

Fig. 4

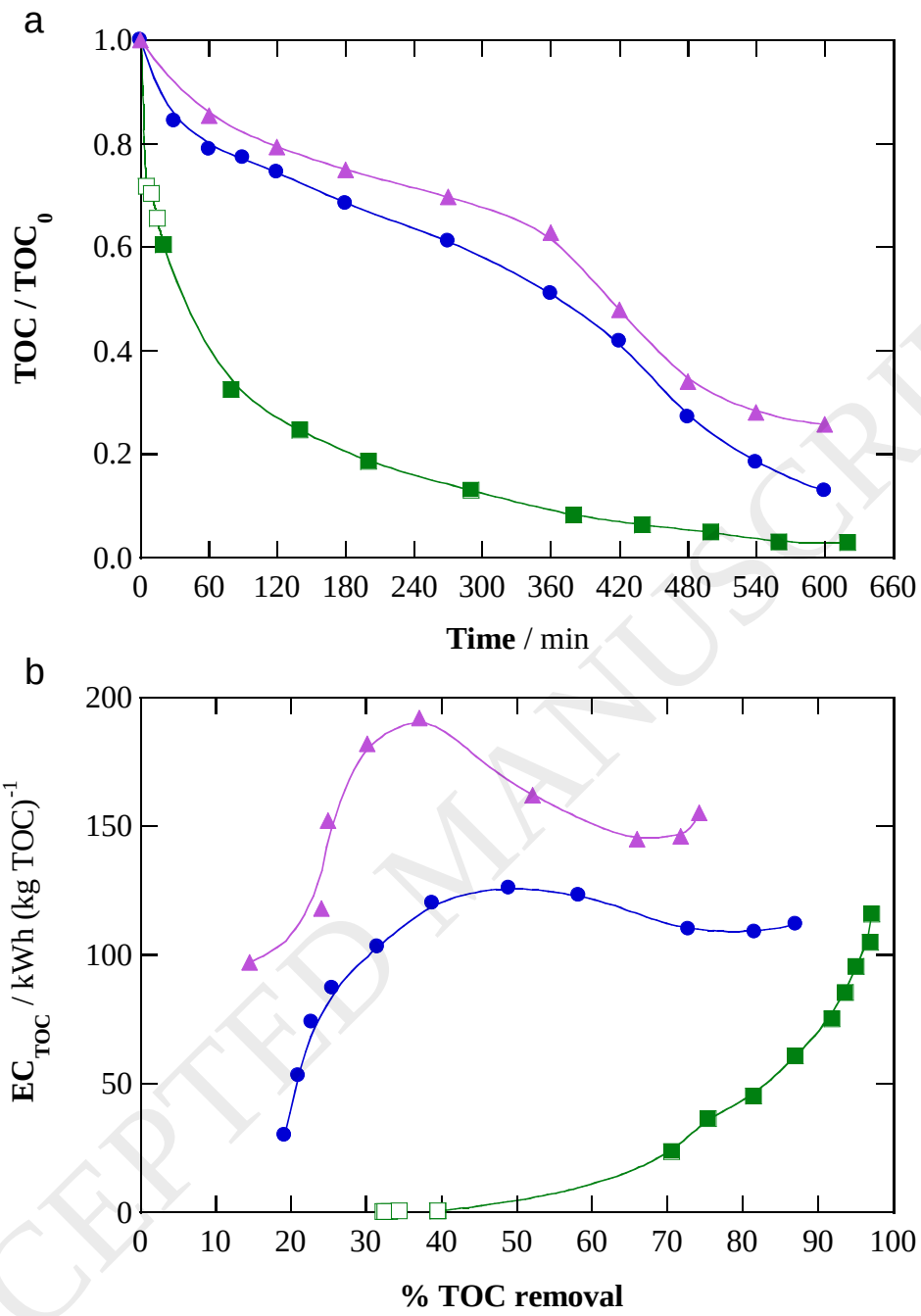

Fig. 5

Table 1

Main physicochemical properties of conditioned OOMW.

Parameter (units)	Value in OOMW sample
pH	6.83±0.07
Conductivity (mS cm^{-1})	3.50
TOC (mg C L^{-1})	581.1±2.3
COD (mg O_2 L^{-1})	1,393.3±.3.0
BOD_5 / COD	0.402
Turbidity (NTU)	191.9±2.0
TS (mg L^{-1})	1,890.0± 0.1
TDS (mg L^{-1})	1,510.1± 0.1
VS (mg L^{-1})	740.2 ±0.1
Total nitrogen (mg N L^{-1})	16.7±0.3
Na^+ (mg L^{-1})	783.2
K^+ (mg L^{-1})	122.4
Ca^{2+} (mg L^{-1})	82.0
Mg^{2+} (mg L^{-1})	63.4
Total iron (mg L^{-1})	0.52
Cl^- (mg L^{-1})	41.8
NO_3^- (mg L^{-1})	0.73
SO_4^{2-} (mg L^{-1})	1558.3

Table 2

Organic components of conditioned OOMW identified by GC-MS using several solvents for extraction and polar or non-polar column for GC separation.

Compound	Solvent [a] (column)	Compound	Solvent [a] (column)
Cyclic compounds (including aromatics)			
1,4-Cyclohexanedione	DCM (P)	Hydroquinone	DCM (P)
Toluene	EA (P, NP)	4-Methylphenylacetic acid	DCM (P), EA (NP)
Ethylbenzene	EA (P)	Benzaldehyde	EA (NP)
p-Xylene	EA (P, NP)	3-Hydroxybenzaldehyde	EA (NP)
1-Propenylbenzene	EA (P)	1-Nitroso-2,4-dymethylaminobenzene	DCM (P)
Phenol	EA (NP)	3,4-Dimethylbenzenamine	DCM (P)
o-(Propylthio)phenol	DCM	3,5-Dihydroxybenzenamide	EA (NP)
4-Methylphenol	DCM (P), EA (P, NP)	1-Ethoxy-4-methylbenzene	DCM (P)
3-Amino-2-methylphenol	EA (NP)	Vanillin	DCM (P)
Aliphatic compounds			
3-Methyl-2-buten-1-ol	DCM (P)	Tetradecanoic acid	DCM (P)
1,2-Ethanediol	DCM (P)	Decanoic acid	DCM (P)
4-(Methylthio)-1-butanethiol	DCM (P)	Nonanoic acid	EA (P), EA (NP)
Hexaethylene glycol	DCM (P)	Heptanoic acid	DCM (P)
Dodecanamide	DCM (P), EA (NP)	4-Hexenoic acid	EA (P)
3-Hydroxyethylbutanoate	DCM (P)	Tartaric acid	EA (P)
Hexadecilhexyl oxalate	DCM (P)	Fumaric acid	DCM (P)
2-Hydroxyethyl disulfide	DCM (P)	(*E*)-2-Butenoic acid	DCM (P)
Dimethyl trisulfide	EA (P)	Malic acid	DCM (P), EA (P)
2-Mercaptopropanoic acid	DCM (P)	Acetic acid	DCM (P)
Oleic acid	DCM (P), EA (NP)	Nonadecane	DCM (P)
Octadecanoic acid	DCM (P), EA (P)	Decane	DCM (P)
Heptadecanoic acid	DCM (P)	Eicosane	DCM (P), EA (NP)
Hexadecanoic acid	DCM (P)		

[a] DCM: dichloromethane, EA: ethyl acetate, P: polar column, NP: non-polar column

Table 3

pH, conductivity, percentage of removal of TOC, COD and turbidity, and specific energy consumption after 45 min of EC of 150 mL of conditioned OOMW using different current densities and electrolytic cells with the same anode and cathode material at 25 ºC.

Electrode material	pH	Conductivity (mS cm^{-1})	% TOC removal	% COD removal	% Turbidity removal	EC_{TOC} (kWh $(kg\ TOC)^{-1}$)
j = 3 mA cm^{-2}						
Al	7.0	2.9	35.1	44.5	98.4	1.9
Fe	6.9	3.5	40.4	43.4	98.4	1.2
AISI 304	7.2	3.1	21.9	33.8	75.7	4.8
AISI 316L	7.1	3.1	21.9	31.1	59.4	5.2
j = 10 mA cm^{-2}						
Al	7.0	3.9	52.4	47.9	99.2	9.7
Fe	7.7	3.5	50.2	46.3	99.3	14.0
AISI 304	8.0	3.5	28.5	44.0	95.7	18.9
AISI 316L	8.0	3.5	24.3	39.0	95.5	26.2
j = 20 mA cm^{-2}						
Al	7.8	3.6	58.6	50.2	99.7	12.7
Fe	8.3	3.5	58.7	49.2	99.4	12.6
AISI 304	8.2	3.6	34.0	41.2	99.8	51.4
AISI 316L	8.1	3.5	28.5	39.8	99.4	71.8
j = 30 mA cm^{-2}						
Al	8.0	3.4	59.8	64.2	98.8	83.1
Fe	9.5	3.3	68.2	64.8	97.6	45.1
AISI 304	8.5	3.5	43.2	47.3	91.6	78.1
AISI 316L	8.2	3.5	29.3	39.9	99.0	127.6

Table 4

pH, conductivity, percentage of removal of TOC, COD and turbidity, and specific energy consumption per unit TOC mass after 45 min of EC of 150 mL of conditioned OOMW using cells with different anode and cathode materials at 30 mA cm^{-2} and 25 ºC.

Anode/Cathode	pH	Conductivity (mS cm^{-1})	% TOC removal	% COD removal	% Turbidity removal	EC_{TOC} (kWh $(kg\ TOC)^{-1}$)
Al/Fe	7.3	2.9	52.3	47.2	99.9	61.2
Al/AISI 304	7.3	3.4	44.2	46.1	99.8	81.5
Al/AISI 316L	7.6	3.2	48.1	46.8	100	62.5
Fe/Al	9.0	3.1	58.0	62.6	98.6	71.9
Fe/AISI 304	9.2	3.3	69.0	65.0	97.8	46.8
Fe/AISI 316L	9.2	3.1	63.9	60.9	99.8	54.9
AISI 304/Al	7.2	3.2	40.5	37.1	99.7	98.6
AISI 304/Fe	8.1	3.3	36.3	34.6	99.7	102.3
AISI 304/AISI 316L	7.6	3.5	32.1	34.6	99.8	112.4
AISI 316L/Al	7.8	3.6	59.7	41.2	99.9	55.6
AISI 316L/Fe	8.2	3.8	44.4	39.0	99.8	81.1
AISI 316L/AISI 304	8.1	3.7	52.8	37.0	99.7	72.0

Table 5

Main physicochemical results after 20 min of EC of 150 mL of conditioned OOMW at pH 6.9 in a Fe/Fe cell at 3 mA cm^{-2} and 25 ºC, followed by EF or PEF post-treatment of 100 mL of the supernatant solution at pH 7.2 using a BDD/air-diffusion cell at 25 mA cm^{-2} and 25 ºC.

Parameter (units)	After 20 min of EC	After 360 min of EF	After 360 min of PEF
% TOC removal	39.5	79.9	80.1
EC_{TOC} (kWh $(kg\ TOC)^{-1}$)	0.5	110.9	119.1
% COD removal	40.4	62.7	60.4
BOD_5/COD	0.404	0.143	0.206
% Turbidity removal	95.0	98.9	98.9
% TS removal	15.1	17.4	- [a]
% Total nitrogen removal	75.6	80.6	78.6
Total iron (mg L^{-1})	2.61	2.31	2.22

[a] Not determined